Ann. of Appl. Math.
36:3(2020), 257-269

UNSTEADY NATURAL CONVECTIVE BOUNDARY LAYER FLOW AND HEAT TRANSFER OF FRACTIONAL SECOND-GRADE NANOFLUIDS WITH DIFFERENT PARTICLE SHAPES[*†]

Ming Shen[‡], Yuhang Wu, Mengchen Zhang

(*College of Mathematics and Computer Science, Fuzhou University, Fuzhou 350108, Fujian, PR China*)

Abstract

The present study is concerned with unsteady natural convective boundary layer flow and heat transfer of fractional second-grade nanofuids for different particle shapes. Nonlinear boundary layer governing equations are formulated with time fractional derivatives in the momentum equation. The governing boundary layer equations of continuity, momentum and energy are reduced by dimensionless variable. Numerical solutions of the momentum and energy equations are obtained by the finite difference method combined with L1-algorithm. The quantites of physical interest are graphically presented and discussed in details. It is found that particle shape, fractional derivative parameter and the Grashof number have profound influences on the the flow and heat transfer.

Keywords second-grade nanofluid; heat transfer; Caputo derivative; particle shape

2000 Mathematics Subject Classification 34K37

1 Introduction

The study of the non-Newtonian fluids has achieved much attention because of well-established applications in a number of processes which occur in industry such as damping and braking devices, personal protective equipment, machining, rocket propellants. The shear stress and shear rate of the non-Newtonian fluids are connected by a relation in a non-linear manner which is generally more complex compared with Newtonian fluid flows. Many research works have been carried out to explore various non-Newtonian fluid flows. Khan et al. [1] studied the heat and

*This research was supported by the Natural Science Foundation of Fujian Province (Grant No.2019J01646).

†Manuscript received April 15, 2019; Revised September 26, 2019

‡Corresponding author. E-mail: shenming0516@fzu.edu.cn

mass flux models on three-dimensional flow of Burgers fluid over a stretching surface. The magnetohydrodynamics (MHD) three-dimensional flow of Oldroyd-B nanofluids was discussed by Hayat et al. [2]. Ramzan et al. [3] studied on the effect of thermal diffusion on the boundary layer flow of mixed convective viscoelastic nanofluids in a porous medium. Alshomrani et al. [4] researched the heat and mass transfer characteristics of steady-state flow of three-dimensional Burgers nanofluids on biaxially stretched surfaces. Bilal et al. [5] investigated the three-dimensional radiation flow of Burgers nanofluids with mass flux effect. Effect of nonlinear radiation on the flow of MHD Carreau nanofluids on a tensile surface with zero mass flux was analyzed by Lu et al. [6]. One of the most popular models for non-Newtonian fluids is the second-grade fluid model which was configured firstly by Coleman and Noll [7]. Subsequently, Bose et al. [8] made a study on Couette flow of second-grade fluid through a porous medium with suction. Exact solutions of a second-grade fluid movement owing to cylinder vibration were presented by Vieru et al. [9]. Jamil and Fetecau [10] discussed exact analytic solutions of rotating flows of a second-grade fluid between cylindrical regions.

Fractional derivatives are better than integer order models in some applications because they can describe the hereditary and memory properties of diverse substances. For example, complex kinetics can be accurately described, and it can also effectively treat viscoelastic properties. The study of fractional derivative models of non-Newtonian fluids generally begins with classical differential equations, which generally use fractional operators instead of integer-order time derivative. Natural convection flow of a second-grade fluid with non-integer order time-fractional derivatives was studied by Imran et al. [11]. With the consideration of Soret and Dufour effects, Zhao et al. [12] introduced the fractional derivative to characterise the natural convection heat and mass transfer of a MHD viscoelastic fluid in a porous medium. Ming et al. [13] derived analytical solutions of a class of new multi-term fractional-order partial differential equations. Rasheed et al. [14] discussed an unsteady flow of an anomalous Oldroyd-B fluid for solving fractional equation. Zhao et al. [15] studied unsteady natural convection heat transfer of generalized Oldroyd-B fluid in a porous medium saturated with modified fractional Darcy's law. Smooth travelling wave solutions of two fractional flow equations from porous media resulting were analyzed by Hönig et al. [16].

The second-grade fluid model is one of the non-Newtonian models, but it is rare to analyze its fractional derivative. This work is aimed to study the natural convection flow of an incompressible fractional second-grade nanofluid near a vertical plate with different particle shapes, and introduce Caputo fractional derivatives into the stress tensor component. The expressions for dimensionless velocity and temperature are solved numerically. The influences of flow parameters as well as the fractional derivative parameter α on the velocity and temperature field are analyzed graphically.

2 Mathematical Formulation of the Problem

Consider the two-dimensional unsteady natural convective boundary layer flow and heat conduction of second-grade nanofluids over a vertical plate. In the cartesian coordinate system, the x-axis is along the upward direction of the plate and the y-axis is perpendicular to the plate. The temperature of the vertical plate and the ambient plate are T_w and T_∞, respectively.

For fractional second-grade fluid model, the stress tensor component τ_{xy} can be described as [17]

$$\tau_{xy} = \mu\frac{\partial u}{\partial y} + \lambda^\alpha D_t^\alpha\Big[\frac{\partial u}{\partial y}\Big], \tag{1}$$

where μ is the effective viscosity, λ is relaxation time, D_t^α is the Caputo fractional derivative and the fractional derivative of order α is defined as [18]

$$D_t^\alpha f(t) = \frac{1}{\Gamma(1-\alpha)}\int_0^t f'(\eta)(t-\eta)^{-\alpha}\mathrm{d}\eta, \tag{2}$$

where Γ is the Gamma function, α is the temperature fractional derivative parameter. Under the boundary layer approximation and the assumption that the viscous dissipation is neglected, the momentum and energy equations for the incompressible flow of a second-grade fluid are

$$\rho_{nf}\Big(\frac{\partial u}{\partial t} + u\frac{\partial u}{\partial x} + v\frac{\partial u}{\partial y}\Big) = \mu_{nf}\Big[\frac{\partial^2 u}{\partial y^2} + \lambda^\alpha D_t^\alpha\Big(\frac{\partial^2 u}{\partial y^2}\Big)\Big] + (\rho\beta)_{nf}g(T-T_\infty), \tag{3}$$

$$(\rho C_p)_{nf}\Big(\frac{\partial T}{\partial t} + u\frac{\partial T}{\partial x} + v\frac{\partial T}{\partial y}\Big) = \kappa_{nf}\frac{\partial^2 T}{\partial y^2}, \tag{4}$$

where u and v are the velocity components along x and y directions respectively, T is temperature, ρ_{nf} is the density of the nanofluid, β_{nf} and $(C_p)_{nf}$ respectively stand for the coefficient of thermal expansion and the specific heat at the constant pressure. μ_{nf} is the viscosity of the nanofluid. Further, the expressions of ρ_{nf}, μ_{nf}, $(\rho\beta)_{nf}$ and $(\rho C_p)_{nf}$ are given [19-22] as follows:

$$\rho_{nf} = (1-\phi)\rho_f + \phi\rho_p, \mu_{nf} = \frac{\mu_f}{(1-\phi)^{2.5}}, \tag{5}$$

$$(\rho\beta)_{nf} = (1-\phi)(\rho\beta)_f + \phi(\rho\beta)_p, (\rho C_p)_{nf} = (1-\phi)(\rho C_p)_f + \phi(\rho C_p)_p, \tag{6}$$

where ϕ is the nanoparticle volume fraction, the subscripts nf, f and p respectively represent the nanofluid, fluid, and nanosolid particles. Moreover, thermal conductivity κ_{nf} is given [23] by

$$\frac{\kappa_{nf}}{\kappa_f}=\frac{(\kappa_p+(m-1)\kappa_f)-(m-1)\phi(\kappa_f-\kappa_p)}{(\kappa_p+(m-1)\kappa_f)+\phi(\kappa_f-\kappa_p)}, \tag{7}$$

where m is the nanoparticle shape factor. The thermophysical properties of the base fluid and nanoparticle are given in Table 1 [24]. Five different types of nanoparticle shapes including sphere, hexahedron, tetrahedron, column and lamina are considered, and the corresponding values of m for the different shapes are shown in Table 2 [25].

Table 1: Physical properties of fluid and nanoparticles

	$\rho(Kgm^{-3})$	$C_p(JKg^{-1}K^{-1})$	$\kappa(Wm^{-1}K^{-1})$	$\beta\times10^{-5}(K^{-1})$
CTAC/NaSal-water	997.1	4179	0.613	21
Cu	8933	385	400	1.67

Table 2: Values of shape factor for different nanoparticle shapes

	Sphere	Hexahedron	Tetrahedron	Column	Lamina
m	3	3.7221	4.0613	6.3698	16.1576

The initial and boundary conditions for this problem are

$$t\le 0: u=0,\ v=0,\ T=T_\infty,\ \text{as } x\ge 0;\quad t>0: u=0,\ v=0,\ T=T_w,\ \text{at } y=0;$$
$$t>0: u\to 0,\ T\to T_\infty,\ \text{as } y\to\infty;\quad t>0: u=0,\ T=T_\infty,\ \text{at } x=0.$$

The dimensionless variables are introduced in the following forms:

$$x^*=\frac{x}{L},\quad y^*=\frac{y}{L}Re^{\frac{1}{2}},\quad t^*=\frac{tU_0}{L},\quad u^*=\frac{u}{U_0},\quad v^*=\frac{v}{U_0}Re^{\frac{1}{2}},\quad \theta=\frac{T-T_\infty}{T_\omega-T_\infty},$$
$$\lambda^*=\frac{\lambda U_0}{L},\quad Pr=\frac{\nu_f}{\alpha_f},\quad \alpha_f=\frac{\kappa_f}{(\rho C_p)_f},\quad \nu_f=\frac{\mu_f}{\rho_f},\quad Re=\frac{U_0L}{\nu_f},$$
$$Gr=\frac{g\beta(T_\omega-T_\infty)L^3}{\nu_f^2},\quad E_1=\frac{1}{(1-\phi)^{2.5}[1-\phi+\phi\frac{\rho_p}{\rho_f}]},\quad E_2=\frac{1-\phi+\phi\frac{(\rho\beta)_p}{(\rho\beta)_f}}{1-\phi+\phi\frac{\rho_p}{\rho_f}},$$
$$H(m,\phi)=\Big[(1-\phi)+\phi\frac{(\rho C_p)_p}{(\rho C_p)_f}\Big]\frac{[\kappa_p+(m-1)\kappa_f]+\phi(\kappa_f-\kappa_p)}{[\kappa_p+(m-1)\kappa_f]-(m-1)\phi(\kappa_f-\kappa_p)},$$

where Re is the generalized Reynolds number, Pr is the Prandtl number, ν is the kinematic viscosity, and Gr is the Grashof number. Omitting the dimensionless mart $*$ for brevity, the governing equations of continuity, momentum and energy can be written as

$$\frac{\partial u}{\partial x}+\frac{\partial v}{\partial y}=0, \tag{8}$$

$$\frac{\partial u}{\partial t}+u\frac{\partial u}{\partial x}+v\frac{\partial u}{\partial y}=E_1\Big[\frac{\partial^2 u}{\partial y^2}+\lambda^\alpha D_t^\alpha\Big(\frac{\partial^2 u}{\partial y^2}\Big)\Big]+\frac{E_2 Gr}{Re^2}\theta, \tag{9}$$

$$\frac{\partial \theta}{\partial t}+u\frac{\partial \theta}{\partial x}+v\frac{\partial \theta}{\partial y}=\frac{1}{Pr\cdot H(m,\phi)}\frac{\partial^2 \theta}{\partial y^2}. \tag{10}$$

The corresponding boundary conditions become

$$t\le 0: u=0,\ v=0,\ \theta=0,\ \text{as } x\ge 0;\quad t>0: u=0,\ v=0,\ \theta=1,\ \text{at } y=0; \tag{11}$$

$$t>0: u\to 0,\ \theta\to 0,\ \text{as } y\to\infty;\quad t>0: u=0,\ \theta=0,\ \text{at } x=0. \tag{12}$$

The physical quantity of interest is the local Nusselt number, which is defined [26] as

$$Nu=\frac{xq_w}{k(T_w-T_\infty)}, \tag{13}$$

where q_w is the heat flux from the flat plate, given by

$$q_w=-k\Big(\frac{\partial T}{\partial y}\Big)_{y=0}. \tag{14}$$

The corresponding dimensionless parameters are given by

$$Nu=-xRe^{\frac{1}{2}}\Big(\frac{\partial \theta}{\partial y}\Big)_{y=0}, \tag{15}$$

Similarly, the average Nusselt number satisfies:

$$\overline{Nu}=-Re^{\frac{1}{2}}\int_0^1\Big(\frac{\partial \theta}{\partial y}\Big)_{y=0}\mathrm{d}x. \tag{16}$$

3 Numerical Techniques

In view of the initial conditions and boundary conditions, the numerical solutions of equations (8)-(10) are defined as $u_{i,j}^k$, $v_{i,j}^k$ and $\theta_{i,j}^k$ at the mesh points (x_i, y_j, t_k). Define $x_i=i\Delta x$ $(i=0,1,2,\cdots,M)$, $y_j=j\Delta y$ $(j=0,1,2,\cdots,N)$ and $t_k=k\Delta t$ $(k=0,1,2,\cdots,R)$, where $\Delta x=L/M$ and $\Delta y=Y_{\max}/N$ are space steps, Δt is time step. Based on the definition of Caputo fractional derivative operate, the time fractional derivative $(0<\alpha<1)$ is discretized by using the L_1-algorithm as [27]

$$D_t^\alpha f(t_k)=\frac{\Delta t^{-\alpha}}{\Gamma(2-\alpha)}\Big[f(t_k)-\alpha_{k-1}f(t_0)-\sum_{s=0}^{k-1}(\alpha_{s-1}-\alpha_s)f(t_{k-s})\Big]+O(\Delta t^{2-\alpha}), \tag{17}$$

where $\alpha_s=(s+1)^{1-\alpha}-s^{1-\alpha}$ $(s=0,1,2,\cdots,R)$. The integer-order terms in the governing equations are discretized as

$$\frac{\partial u}{\partial t}\Big|_{t=t_k} = \frac{u(x_i,y_j,t_k)-u(x_i,y_j,t_{k-1})}{\Delta t} + O(\Delta t), \tag{18}$$

$$u\frac{\partial u}{\partial x}\Big|_{t=t_k} = u(x_i,y_j,t_{k-1})\frac{u(x_i,y_j,t_k)-u(x_{i-1},y_j,t_k)}{\Delta x} + O(\Delta x+\Delta t), \tag{19}$$

$$v\frac{\partial u}{\partial y}\Big|_{t=t_k} = v(x_i,y_j,t_{k-1})\frac{u(x_i,y_j,t_k)-u(x_i,y_{j-1},t_k)}{\Delta y} + O(\Delta y+\Delta t), \tag{20}$$

$$\frac{\partial^2 u}{\partial y^2}\Big|_{t=t_k} = \frac{u(x_i,y_{j+1},t_k)-2u(x_i,y_j,t_k)+u(x_i,y_{j-1},t_k)}{\Delta y^2} + O(\Delta y^2), \tag{21}$$

$$\frac{\partial^2 \theta}{\partial y^2}\Big|_{t=t_k} = \frac{\theta(x_i,y_{j+1},t_k)-2\theta(x_i,y_j,t_k)+\theta(x_i,y_{j-1},t_k)}{\Delta y^2} + O(\Delta y^2). \tag{22}$$

For simplicity, note

$$r_1=\frac{E_1\Delta t}{\Delta y^2},\quad r_2=\frac{\Delta t}{\Delta y^2},\quad r_3=\frac{\lambda^\alpha\Delta t^{-\alpha}}{\Gamma(2-\alpha)},\quad C=\sum_{s=1}^{k-1}(\alpha_{s-1}-\alpha_s)\delta_y^2u_{i,j}^{k-s},$$

where $\delta_y^2u_{i,j}^{k-s}=u_{i,j+1}^{k-s}-2u_{i,j}^{k-s}+u_{i,j-1}^{k-s}$.

Finally, the iteration equations are achieved as follows:

$$\begin{aligned}&-\frac{\Delta t}{\Delta x}u_{i,j}^{k-1}\theta_{i-1,j}^k-\Big(\frac{\Delta t}{\Delta y}v_{i,j}^{k-1}+\frac{r_2}{Pr\cdot H(m,\phi)}\Big)\theta_{i,j-1}^k+\Big(1+\frac{\Delta t}{\Delta x}u_{i,j}^{k-1}\\&+\frac{\Delta t}{\Delta y}v_{i,j}^{k-1}+\frac{2r_2}{Pr\cdot H(m,\phi)}\Big)\theta_{i,j}^k-\frac{r_2}{Pr\cdot H(m,\phi)}\theta_{i,j+1}^k=\theta_{i,j}^{k-1},\end{aligned} \tag{23}$$

$$\begin{aligned}&-\frac{\Delta t}{\Delta x}u_{i,j}^{k-1}u_{i-1,j}^k-\Big(\frac{\Delta t}{\Delta y}v_{i,j}^{k-1}+r_1(1+r_3)\Big)u_{i,j-1}^k+\Big(1+\frac{\Delta t}{\Delta x}u_{i,j}^{k-1}+\frac{\Delta t}{\Delta y}v_{i,j}^{k-1}\\&+2r_1(1+r3)\Big)u_{i,j}^k-r_1(1+r_3)u_{i,j+1}^k=u_{i,j}^{k-1}-r_1r_3C+\frac{E_2Gr}{Re^2}\theta_{i,j}^k,\end{aligned} \tag{24}$$

$$v_{i,j}^k=v_{i,j-1}^k-\frac{\Delta y}{\Delta x}(u_{i,j}^k-u_{i-1,j}^k). \tag{25}$$

4 Results and Discussion

Iteration equations (23)-(25) can be written in the tri-diagonal systems, which were solved by the Thomas algorithm [28]. The iteration tends to be stable when the interpolation between u and θ is less than 10^{-5} at two adjacent time steps. The calculation area can be seen as a rectangle with $x_{\max}=2$ and $y_{\max}=8$, where $y_{\max}$ corresponds to $y\to\infty$. In the calculation process, the space and time steps are fixed as $\Delta x=0.02$, $\Delta y=0.08$ and $\Delta t=0.15$. As shown in Figure 1, the resulting numerical solution is stable and convergent by comparing u and θ of different grid sizes.

It is revealed from Figure 2 that the nanoparticle shape has a significant impact on temperature and heat transfer of the nanofluid. It can be observed that temperature profile declines uniformly with the decreasing of m. The results imply that sphere < hexahedron < tetrahedron < column < lamina for the thickness of thermal boundary layer, so the sphere nanoparticle has the best heat conduction among the five different shapes. Figures 3 and 4 illustrate the effect of α on the velocity and temperature profiles. The increasing α leads to a obvious increase of the velocity before the turning point as shown in Figure 3, then intersects at a point after the turning point. Therefore, the boundary layer thickness becomes thinner as α evolves after the intersection point. Appearance of the intersection point implies that the fractional equation with relaxation time has temporary memory characteristics with apparent state and response to the outside. From Figure 4, it is easy to see that the decreasing α results in the increase of temperature and the boundary layer.

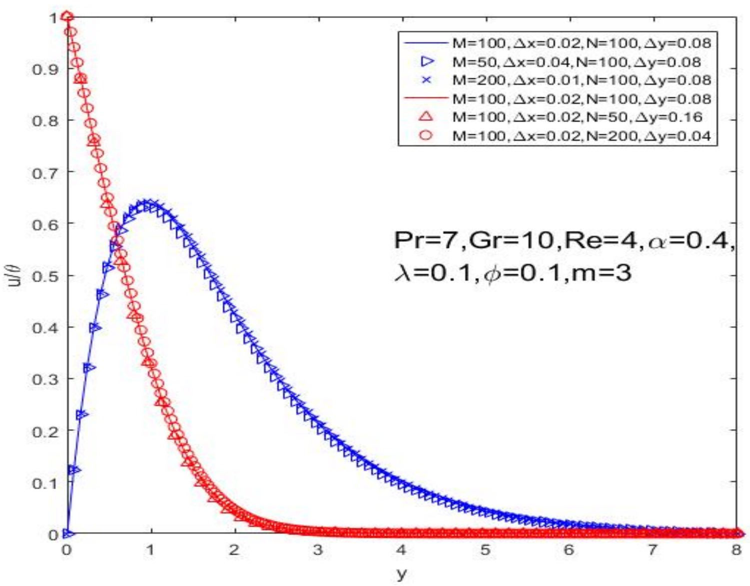

Figure 1: Grid independence test for different mesh sizes

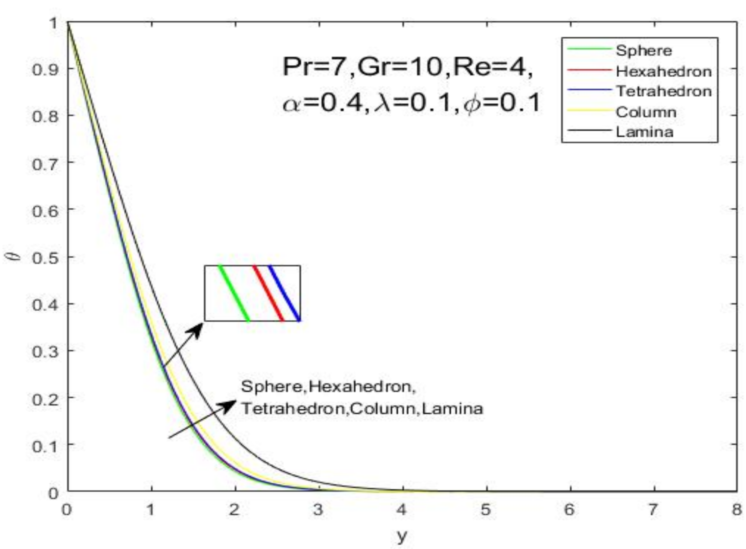

Figure 2: Influence of shapes on temperature profiles

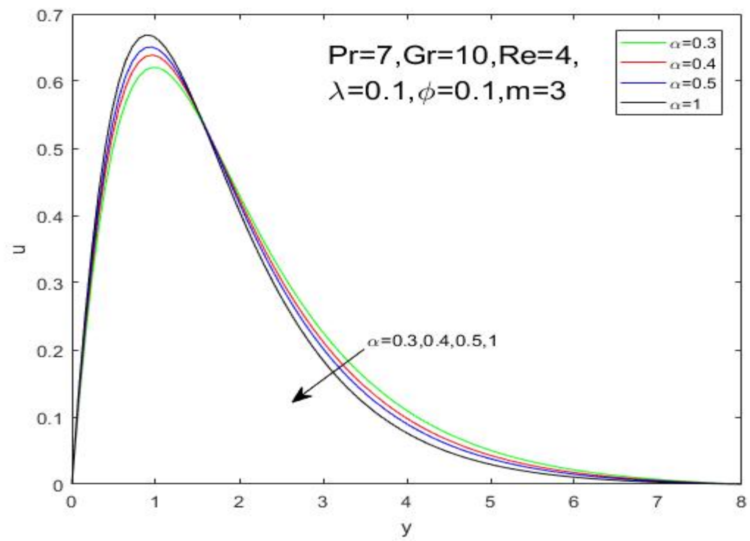

Figure 3: Influence of α on velocity profiles

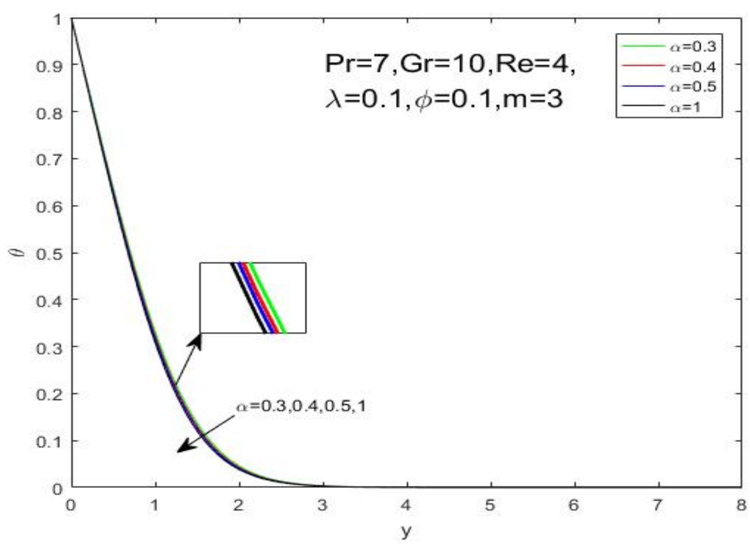

Figure 4: Influence of α on temperature profiles

The influence of ϕ on the velocity and temperature profiles are illustrated in Figures 5 and 6. It is observed from Figure 5 that the maximum values of the velocity profiles reduce as the nanoparticle volume fraction ϕ rises, because the nanoparticles are solid particles, which bring the additional flow resistance. As shown in Figure 6, it can be observed that the temperature and thermal boundary layer thickness increase as ϕ rises. These phenomenons indicate that an increase in the number of nanoparticles weakens heat and momentum transfer of fluid.

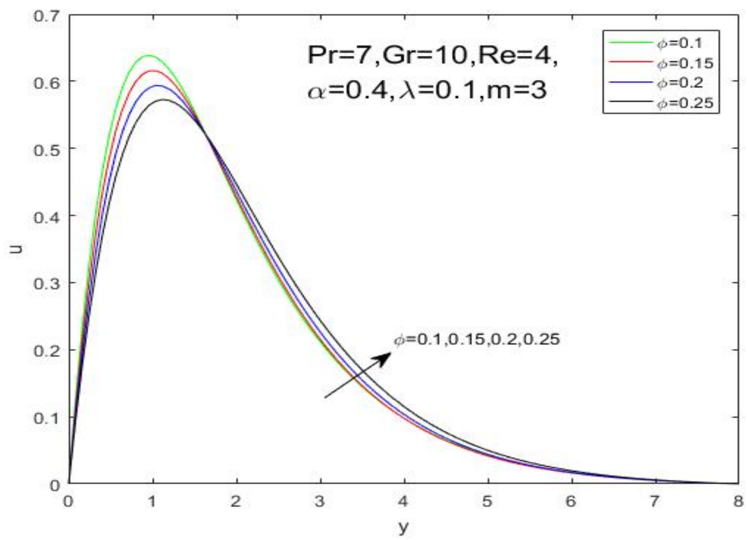

Figure 5: Influence of ϕ on velocity profiles

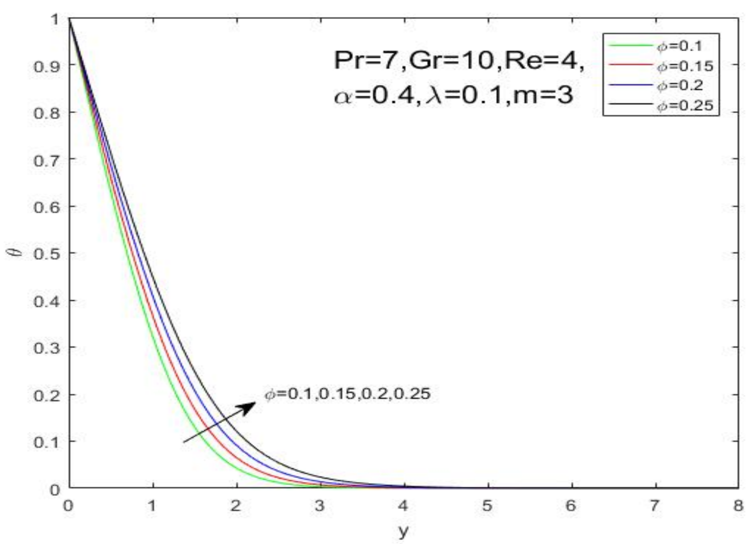

Figure 6: Influence of ϕ on temperature profiles

The Grashof number approximates the ratio of buoyancy to viscous forces acting on the fluid. The impacts of the Grashof number on velocity and temperature profiles are respectively shown in Figures 7 and 8. It is found that the maximum value of the fluid velocity rises as the Grashof number rises as shown in Figure 7. However, the values of temperature and the thermal boundary layer thickness diminish as Gr evolves. This is due to the fact that the parameter Gr is a non-dimensional physical quantity to reflect buoyancy on the fluid, which provides the power of flow.

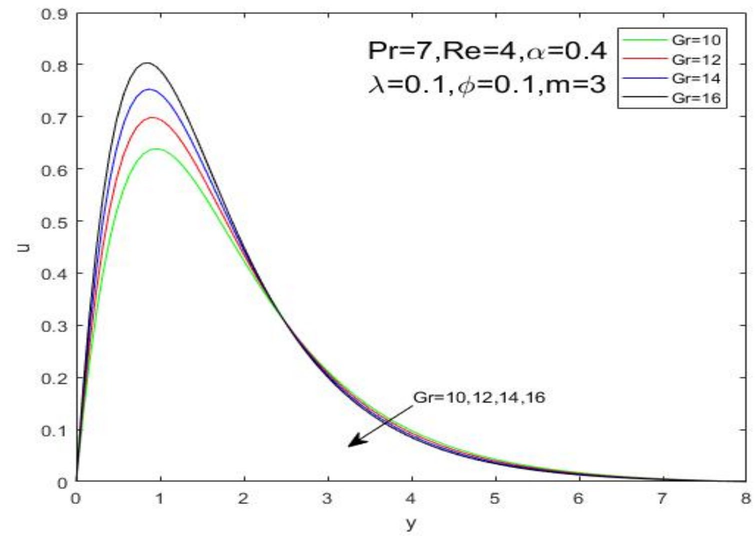

Figure 7: Influence of Gr on velocity profiles

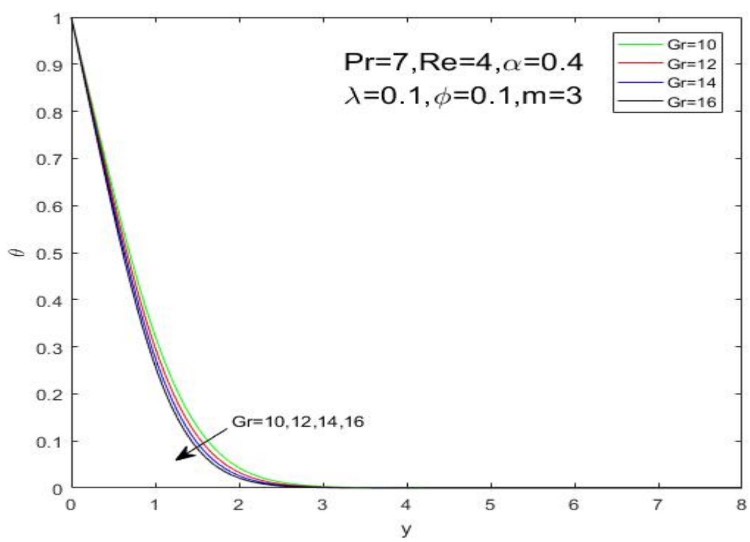

Figure 8: Influence of Gr on temperature profiles

The average Nusselt number is an important physical quantity to investigate the heat transfer of the flow. The impact of m on the average Nusselt number is displayed in Figure 9. This result indicates that sphere > hexahedron > tetrahedron> column > lamina for the average Nusselt number. It is due to the fact that the ratio of thermal conductivity κ_{nf}/κ_f increases with m. The value of the average Nusselt number for the sphere nanoparticle is the largest among the five different shapes, which is in accordance with the results illustrated by Figure 2. It is worth noting that the average Nusselt number drops rapidly first and then slowly rises until it stabilizes.

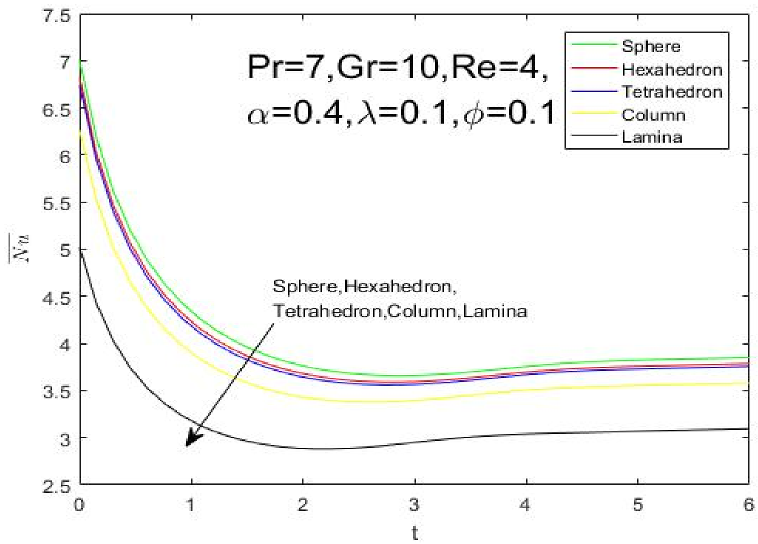

Figure 9: Influence of shapes on the Average Nusselt number

5 Conclusion

The paper is concerned with the natural convection flow of a fractional second-grade nanofluid. The effects of nanoparticle shapes on the flow and heat transfer are probed in this paper. The worth mentioning points are obtained as follows:

1) Sphere nanoparticle has the minimum thermal boundary layer thickness and the maximum average Nusselt number. Therefore, the heat transfer of spherical nanoparticles is superior to other nanoparticles.

2) The velocity increases with y before reaching the maximum values with the impact of α. Then the velocity profiles intersect at a point after the turning point, which implies the fractional nanofluids model with Caputo time derivatives has a short memory of previous states.

3) The nanoparticle volume fraction ϕ has an opposite effect on temperature and velocity profiles. The maximum values of the velocity profiles reduce as the nanoparticle volume fraction ϕ rises because solid particles bring the additional flow resistance.

4) The Grashof number has a similar influence on velocity and temperature profiles with α. The values of temperature and the thermal boundary layer thickness diminish as Gr evolves because of the thermal buoyancy effect.

References

[1] W.A. Khan, M. Khan, A.S. Alshomrani, Impact of chemical processes on 3D Burgers fluid utilizing Cattaneo-Christov double-diffusion: Applications of non-Fouriers heat and non-Ficks mass flux models, *J. Mol. Liq.*, **223**(2016),1039-1047.

[2] T. Hayat, T. Muhammad, S.A. Shehzad, A. Alsaedi, An analytical solution for magnetohydrodynamic Oldroyd-B nanofluid flow induced by a stretching sheet with heat generation/absorption, *Int. J. Therm. Sci.*, **111**(2017),274-288.

[3] M. Ramzan, Farhan Yousaf, M. Farooq, J.D. Chung, Mixed convective viscoelastic nanofluid flow past a porous media with soretdufour effects, *Commun. Theor. Phys.*, **66**(2016),133-142.

[4] M. Khan, W.A. Khan, A.S. Alshomrani, Non-linear radiative flow of three-dimensional Burgers nanofluid with new mass flux effect, *Int. J. Heat Mass Transfer.*, **101**(2016), 570-576.

[5] M. Ramzan, M. Bilal, J.D. Chung, Radiative Williamson nanofluid flow over a convectively heated Riga plate with chemical reaction-A numerical approach, *Chinese J. Phys.*, **55**(2017),1663-1673.

[6] D. Lu, M. Ramzan, N. Huda, J.D. Chung, U. Farooq, Nonlinear radiation effect on MHD Carreau nanofluid flow over a radially stretching surface with zero mass flux at the surface, *Sci. Rep.*, **8**(2018),3709.

[7] B.D. Coleman, W. Noll, An approximation theorem for functionals, with applications in continuum mechanics, *Arch. Ration. Mech. Anal.*, **6**(1960),355-370.

[8] Dhiman Bose, Uma Basu, Unsteady couette flow of a generalized second grade fluid through a porous medium with uniform injection and suction, *IOSR-JM*, **11**(2015),14-19.

[9] D. Vieru, W. Akhtar, C. Fetecau, Starting solutions for the oscillating motion of a Maxwell fluid in cylindrical domains, *Meccanica*, **42**(2007),573-583.

[10] M. Jamil, C. Fetecau, Some exact solutions for rotating flows of a generalized Burgers fluid in cylindrical domains, *J. Non-Newtonian Fluid Mech.*, **165**(2010),1700-1712.

[11] M.A. Imran, I. Khan, M. Ahmad, N.A. Shah, M. Nazar, Heat and mass transport of differential type fluid with non-integer order time-fractional caputo derivatives, *J. Mol. Liq.*, **229**(2017),67-75.

[12] J. Zhao, L. Zheng, X. Zhang, F. Liu, Convection heat and mass transfer of fractional MHD maxwell fluid in a porous medium with soret and dufour effects, *Int. J. Heat Mass Transf.*, **103**(2016),203-210.

[13] C. Ming, F. Liu, L. Zheng, I. Turner, V. Anh, Analytical solutions of multi-term time fractional differential equations and application to unsteady flows of generalized viscoelastic fluid, *Comput. Math. Appl.*, **72**(2016),2084-2097.

[14] A. Rasheed, A. Wahab, S.Q. Shah, R. Nawaz, Finite difference-finite element approach for solving fractional oldroyd-b equation, *Advan. Diff. Eq.*, **2016**(2016),236-257.

[15] J. Zhao, L. Zheng, X. Zhang, F. Liu, X. Chen, Unsteady natural convection heat transfer past a vertical flat plate embedded in a porous medium saturated with fractional oldroyd-b fluid, *J. Heat Transf.*, **139**(2017),012501.

[16] O. Hönig, P.A. Zegeling, F. Doster, R. Hilfer, Non-monotonic travelling wave fronts in a system of fractional flow equations from porous media, *Transf Porous Med.*, **114**(2016),309-340.

[17] X. Wang, H. Qi, B. Yu, Z. Xiong, H. Xu, Analytical and numerical study of electroosmotic slip flows of fractional second grade fluids, *Commun. Nonlinear Sci. Numer. Simulat.*, **50**(2017),77-87.

[18] I. Podlubny, Fractional Differential Equations, Academic Press, San Diego, 1999.

[19] Abu-Nada, Application of nanofluids for heat transfer enhancement of separated flows encountered in a backward facing step, *International Journal of Heat and Fluid Flow*, **29**(2008),242-249.

[20] H.C. Brinkman, The Viscosity of Concentrated Suspensions and Solutions, *The Journal of Chemical Physics*, **20**(1952),571-571.

[21] A. Malvandi, F. Hedayati, D.D. Ganji, Slip effects on unsteady stagnation point flow of a nanofluid over a stretching sheet, *Powder Technol.*, **253**(2014),377-384.

[22] M. Sheikholeslami, D.D. Ganji, H.R. Ashorynejad, Investigation of squeezing unsteady nanofluid flow using ADM, *Powder Technol.*, **239**(2013),259-265.

[23] R.L. Hamilton, O.K. Crosser, Thermal conductivity of heterogeneous two-component system, *I&EC Fundamentals*, **1**(1962),187-191.

[24] Z. Cao, J. Zhao, Z. Wang, F. Liu and L. Zheng, MHD flow and heat transfer of fractional Maxwell viscoelastic nanofluid over a moving plate, *Journal of Molecular Liquids*, **222**(2016),1121-1127.

[25] Y. Lin, B. Li, L. Zheng, G. Chen, Particle shape and radiation effects on Marangoni boundary layer flow and heat transfer of copper-water nanofluid driven by an exponential temperature, *Power Technology*, **301**(2016),379-386.

[26] M. Sajid, I. Ahmad, T. Hayat, M. Ayub, Unsteady flow and heat transfer of a second grade fluid over a stretching sheet, *Communications in Nonlinear Science and Numerical Simulation*, **14**(2009),96-108.

[27] F. Liu, P. Zhuang, V. Anh, I. Turner, K. Burrage, Stability and convergence of the difference methods for the space-time fractional advection-diffusion equation, *Appl. Math. Comput.*, **191**(2007),12-20.

[28] B. Carnahan, H.A. Luther, J.O. Wilkes, Applied Numerical Methods, John Wiley and Sons, 1969.

(*edited by Mengxin He*)